

人工股骨头置换术中置入不同直径假体球头的有限元分析

王学斌¹, 庞清江², 余霄²

(1. 宁波大学医学院, 浙江 宁波 315211; 2. 中国科学院大学宁波华美医院, 浙江 宁波 315010)

【摘要】 目的: 针对老年股骨颈骨折行人工股骨头置换术中, 借助三维有限元分析的方法, 探讨置入不同直径的假体球头后的髋关节生物力学变化, 观察对髋关节应力分布变化, 以便选择出合适的假体球头尺寸。方法: 利用薄层 CT 资料及人工股骨头假体相关参数建立装配有不同假体球头直径的人工股骨头置换术后髋关节有限元模型(M0: 术前模型; M1: 球头直径=原股骨头直径; M2: 球头直径=原股骨头直径+1 mm; M3: 球头直径=原股骨头直径-1 mm; M4: 球头直径=原股骨头直径-2 mm), 并加载关节合力及相关肌肉的负荷, 模拟人缓慢行走时单足站立状态, 分析不同直径假体植入后髋臼周围骨质及软骨的应力分布及变化。结果: (1) M1~M4 中骨盆均出现了不同程度的应力集中, M3 的骨盆 Von Mises 应力峰值为 44.8 MPa, 与术前最为接近, 增量约 13.4%, 且 M3 的骨盆位移在术后 4 组模型中最小, 为 1.40 mm; 其次是 M1, 应力峰值为 47.3 MPa, 增量约 19.7%, 骨盆位移为 1.59 mm。(2) 在髋臼区域, M3 的 Von Mises 应力峰值为 23.3 MPa, 与术前最为接近, 增量约 6.3%, 其次是 M1, 应力峰值为 24.0 MPa, 增量约 8.1%。(3) 髋臼软骨上, M1 与 M3 的应力分布同术前相似, 且 M3 的 Von Mises 应力峰值为 18.5 MPa, 与术前最为接近; 其次是 M1, 应力峰值为 22.5 MPa。(4) M1~M4 均在人工股骨头的外上象限出现不同程度的应力集中, 而在其下方表现为应力遮挡; 其中 M3 的 Von Mises 应力分布较其余模型更为均匀, 其峰值 70.8 MPa 为各组中最低, 其次为 M1(80.7 MPa)。结论: 在行人工股骨头置换术时, 建议优先使用比原股骨头直径小 1 mm 的假体球头, 其次是与原股骨头直径相等的假体球头, 来获得与置换术前的髋关节最接近的自然力学特性, 降低因尺寸差异导致的并发症风险。

【关键词】 髋假体; 关节成形术, 置换; 股骨头; 有限元分析

中图分类号: R683

DOI: 10.12200/j.issn.1003-0034.2020.06.014

开放科学(资源服务)标识码(OSID):



Finite element analysis of different diameter prosthesis ball head in artificial femoral head replacement WANG Xue-bin, PANF Qing-jiang*, and YU Xiao. Huamei Hospital, University of Chinese Academy of Science, Ningbo 315010, Zhejiang, China

ABSTRACT Objective: In order to select the proper size of prosthesis ball head, the biomechanical changes of hip joint using different diameter prosthesis ball head was studied by three-dimensional finite element analysis. **Methods:** The thin-layer CT data and related parameters of artificial femoral head prosthesis were used to establish the finite element model of hip joint after artificial femoral head replacement with different ball diameter of prosthesis(M0: preoperative model; M1: ball head diameter=original femoral head diameter; M2: ball head diameter=original femoral head diameter+1 mm; M3: Ball head diameter=Original femoral head diameter -1 mm; M4: ball head diameter=original femoral head diameter-2 mm). Loading the joint forces and related muscle loads were loaded, and the stress distribution and change of bone and cartilage around acetabulum were analyzed by simulating the standing state of one foot when walking slowly. **Results:** (1) In M1 to M4, the stress concentration in pelvis was different. The peak value of Von Mises stress in the pelvis of M3 was 44.8 MPa, which was the closest to that before operation, with an increment of 13.4%. The displacement of the pelvis of M3 was the smallest in the four groups after operation, with an increment of 1.40 mm. The next was M1, with a peak value of 47.3 MPa, with an increment of 19.7%, and a pelvic displacement of 1.59 mm. (2) In acetabulum area, the peak value of Von Mises stress in M3 was 23.3 MPa, which was the closest to that before operation, with an increment of about 6.3%, followed by M1, with a peak value of 24.0 MPa and an increment of about 8.1%. (3) On the acetabulum cartilage, the stress distribution of M1 and M3 was similar to that before opera-

基金项目: 浙江省医药卫生科技资助项目(编号:2018KY156); 宁波市自然科学基金(编号:2019A610242); 中国科学院大学宁波华美医院“华美研究基金”(编号:2020HMKY18)

Fund program: Zhejiang Medical Science and Technology Funding Project(No. 2018KY156)

通讯作者: 庞清江 E-mail: pqjey@sina.com

Corresponding author: PANG Qing-jiang E-mail: pqjey@sina.com

tion, and the peak value of Von Mises stress of M3 was 18.5 MPa, which was the closest to that before operation, followed by M1, which was 22.5 MPa. (4) M1 to M4 showed different degree of stress concentration in the outer upper quadrant of the artificial femoral head, but showed stress shielding under it; among them, the von Mises stress distribution of M3 was more uniform than that of other models, and its peak value (70.8 MPa) was the lowest in each group, followed by M1 (80.7 MPa). **Conclusion:** When femoral head replacement is performed, it is suggested that the prosthesis ball head with the diameter less than 1 mm and the prosthesis ball head with the same diameter as the original femoral head should be used first, so as to obtain the closest natural mechanical characteristics of the hip joint before the replacement and reduce the risk of complications caused by size differences.

KEYWORDS Hip prosthesis; Arthroplasty, replacement; Femur head; Finite element analysis

股骨颈骨折是老年人最常见的骨折之一，多选用人工髋关节置换术以恢复患者的日常生活能力和行走能力，提高老年患者的生活质量，对于高龄、基础疾病多、术后生活质量要求低、主要限于室内活动的老年患者，人工股骨头置换术可作为首选的治疗方案^[1-2]。但人工股骨头置换术中，由于自身特性引起的一种并发症是髋臼磨损。造成髋臼磨损的原因除了肥胖超重、已有的髋臼病变或损伤、术后活动量大小等因素外，还与股骨头假体直径过大或过小^[3]有关。为了寻找能获得与术前髋关节应力状态最接近的假体球头直径，为了给术后髋臼磨损、髋关节功能受限、髋关节骨性关节炎等相关并发症提供生物力学依据，也为临床上人工股骨头直径选择提供理论参考和指导，笔者拟借助有限元分析的方法，对不同直径的假体球头置换后髋臼区域应力分布情况、位移进行力学比较。

1 资料与方法

1.1 CT 三维重建髋关节

选择 75 岁男性 1 名，体重 70 kg，影像检查及临床已排除畸形、无基础疾病且髋关节结构正常、无创伤及手术史，行髋关节薄层 CT 扫描，将 CT 扫描图像数据导入 Mimics 16.0 软件中，确定坐标轴方向。依据 CT 的灰度值提取骨轮廓，分为皮质骨和松质骨，最后得到髋关节三维几何模型。

1.2 建立正常髋关节有限元模型

对 Mimics 16.0 软件导出的数据进行三角面片细分，降噪，光顺化处理，并通过精确曲面等过程对其进行曲面化，最终形成正常髋关节三维实体模型(编号:M0)。

1.3 建立装配有不同直径假体球头的术后髋关节有限元模型

参照人工股骨头假体的实体和设计模板，测出与股骨相匹配的标准假体柄及 4 种不同型号的股骨头假体(M1:球头直径=原股骨头直径;M2:球头直径=原股骨头直径+1 mm;M3:球头直径=原股骨头直径-1 mm;M4:球头直径=原股骨头直径-2 mm)进行参数化建模。

本试验测得患者股骨头最大直径为 48 mm。即 M1=48 mm;M2=49 mm;M3=47 mm;M4=46 mm。

按照人工股骨头置换术的标准对股骨模型进行截骨处理:截骨线内缘在小转子上 1 cm,外缘到达大转子窝转向其内面，假体柄的轴线与股骨干的轴线重合一致。并根据健侧测得的股骨头旋转中心相对位置及前倾角度进行假体的安装。设定假体与骨的摩擦因数为 0.3^[4]，假体与骨骼紧密压配，模拟稳定骨长如后的界面状态，分别安装上述 4 组人工股骨头假体。

1.4 划分有限元网格及材料参数

将正常髋关节模型、4 组人工股骨头假体模型结构模型 STP 文件导入 Hypermesh 13.0 软件中进行网格划分(表 1),导出 BDF 格式文件,最后参考已发表研究数据^[4-5],在 MSC.Patran 2012 软件中进行材料参数设置(表 2),股骨假体柄采用钛合金(Ti-6Al-7Nb)材料,人工股骨头假体采用钴铬钼合金材料。

表 1 不同直径假体球头的术后髋关节有限元模型各组成有限元网格数量

Tab.1 Finite element mesh number of each group of hip joint finite element model with prosthesis ball head of different diameter

| 组别 | 说明 | 节点数量(个) | 单元数量(个) |
|----|-------------|---------|---------|
| M0 | 股骨头直径=48 mm | 66 055 | 322 319 |
| M1 | 假体头直径=48 mm | 69 540 | 341 948 |
| M2 | 假体头直径=49 mm | 69 409 | 341 932 |
| M3 | 假体头直径=47 mm | 68 549 | 336 102 |
| M4 | 假体头直径=46 mm | 68 666 | 337 308 |

1.5 边界约束及载荷材料参数

假定股骨上段下端固定约束，对股骨远端面上所有节点限制其 6 个方向的自由度；在髋髂关节、耻骨联合处设置一定的水平约束，仅限制其水平方向的自由度，不限制竖向位移和转动的功能；假定骨结构、软骨为连续、均匀、各向同性的线弹性材料；参考 Wei 等^[6]有限元分析时采用的一种较精确的简化受

表 2 不同直径假体球头的术后髋关节有限元模型各组模型对应的材料参数

Tab.2 Material parameters of each group of hip joint finite element models with prosthesis ball head of different diameter

| 结构组织 | 弹性模量(MPa) | 泊松比 |
|----------------|-----------|------|
| 皮质骨 | 10 117 | 0.30 |
| 松质骨 | 151 | 0.22 |
| 股骨假体柄(钛合金) | 110 000 | 0.30 |
| 人工股骨头假体(钴铬钼合金) | 210 000 | 0.30 |
| 股骨头软骨 | 11.85 | 0.45 |
| 髌臼软骨 | 11.85 | 0.45 |

力模型进行分析(图 1),固定股骨远段,在骨盆髌髌关节及耻骨联合上的节点共施加向下 600 N 的力,来模拟缓慢行走时人体单脚站立时股骨头处所承受的主要负荷,并在大转子施加 2 582 N 的力模拟外展肌的肌力。

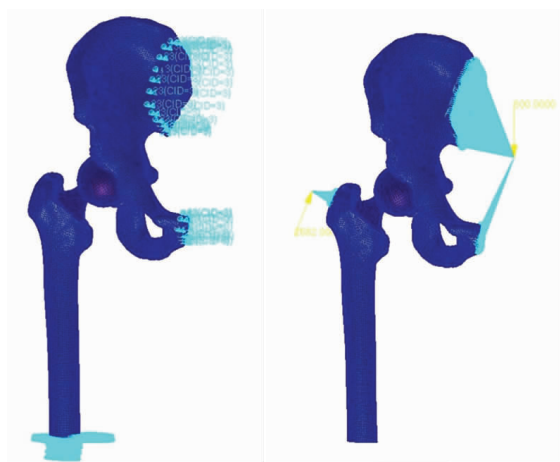


图 1 (M1~M4)模型边界约束及载荷

Fig.1 Boundary constraint and load of (M1 to M4) model

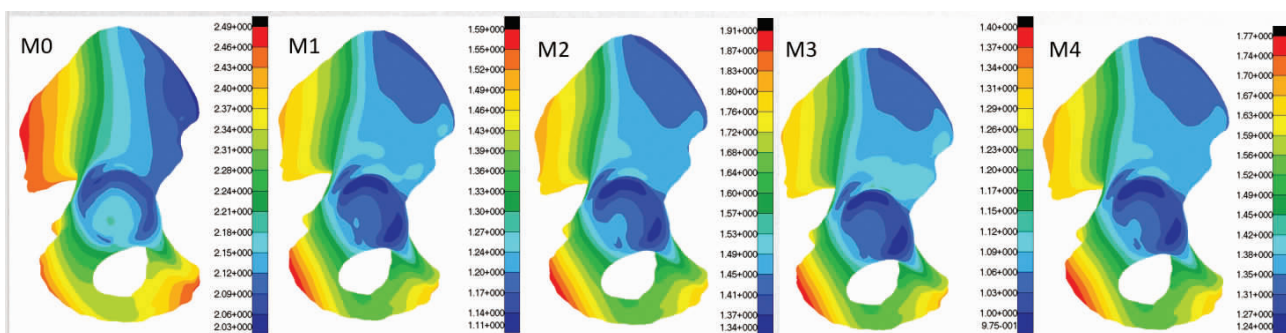


图 2 不同直径假体球头置入后骨盆位移图。M0:原股骨头置入时最大位移为 2.49 mm;M1:48 mm 球头置入时最大位移为 1.59 mm;M2:49 mm 球头置入时最大位移为 1.91 mm;M3:47 mm 球头置入时最大位移为 1.40 mm;M4:46 mm 球头置入时最大位移为 1.77 mm

Fig.2 Pelvic displacement after ball head placement of prosthesis with different diameters. M0:the maximum displacement was 2.49 mm after replacement of the original femoral head;M1:the maximum displacement was 1.59 mm after replacement of the ball head with 48 mm diameter;M2:the maximum displacement was 1.91 mm after replacement of the ball head with 49 mm diameter;M3:the maximum displacement was 1.40 mm after replacement of the ball head with 47 mm diameter;M4:the maximum displacement was 1.77 mm after replacement of the ball head with 46 mm diameter

1.6 观测指标

对所建模型进行有效性验证后,观察并比较各组在骨性髌臼、髌臼软骨的 Von Mises 应力云图、位移和等效应变云图,并求得最大 Von Mises 应力、最大位移和最大等效应变值。

2 结果

2.1 各模型骨盆位移及应力分布变化

设定一定的约束边界后,骨盆在受到力学加载时可能会出现沿冠状面或矢状面的位移,从而会影响到关节的力学环境。由图 2 可见各模型的位移情况,在此种载荷条件下骨盆的最大位移出现在髌骨翼后部及坐骨结节处,相比于 M0 模型,M1~M4 对应的位移峰值均有所下降,降幅约在-44%~-23%,其中以 M3 模型(球头直径=47 mm)位移最小,为 1.40 mm;其次是 M1 模型(球头直径=48 mm),位移 1.59 mm。

各模型骨盆的 Von Mises 应力分布云图见图 3,应力集中区域为髌骨翼下方接近坐骨大切迹处。置换为弹性模量较大的假体球头后,各模型在该区域的应力均出现不同程度的增大趋势,其中 M3(球头直径=47 mm)的应力峰值为 44.8 MPa,与术前最为接近,增量约 13.4%;其次是 M1(球头直径=48 mm),应力峰值为 47.3 MPa,增量约 19.7%;而 M2(球头直径=49 mm)应力峰值最大,达到 54.2 MPa,增幅为 37.21%。

2.2 各模型髌臼及髌臼软骨的 Von Mises 应力分布

通过应力云图(图 4)可见,置换前髌臼应力峰值出现在顶部偏后上方区域,置换后其移至髌臼顶部,且偏中心处亦出现不同程度的应力集中,对比术前 M0(22.2 MPa),M1~M4 的最大 Von Mises 应力在 20.1~25.1 MPa 间,其中 M2(球头直径=48 mm)呈现应力分散,峰值降为 20.1 MPa;M4(球头直径=46 mm)应力峰值最大,为 25.1 MPa,且出现在中心区;

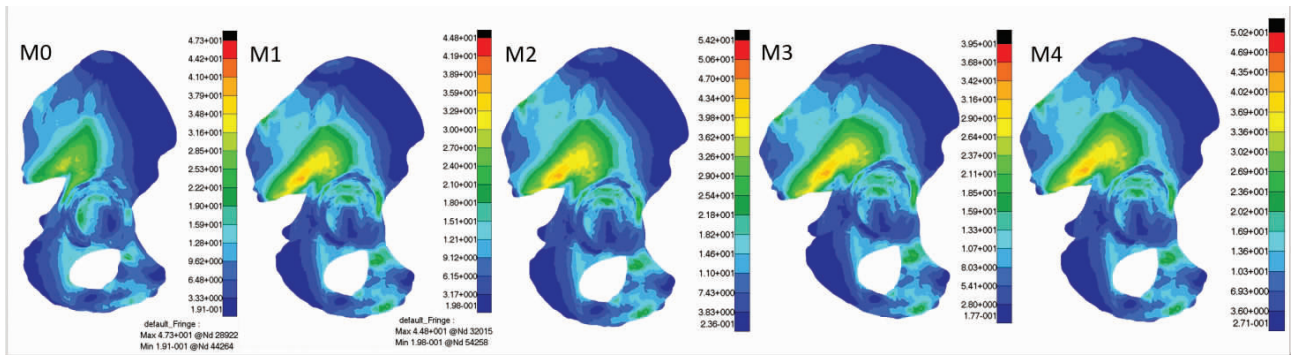


图 3 不同直径假体球头置入后骨盆 Von Mises 应力分布云图。M0:原股骨头置入时应力峰值为 39.5 MPa;M1:48 mm 球头置入时应力峰值为 47.3 MPa;M2:49 mm 球头置入时应力峰值为 54.2 MPa;M3:47 mm 球头置入时应力峰值为 44.8 MPa;M4:46 mm 球头置入时应力峰值为 50.2 MPa

Fig.3 Cloud chart of Von Mises stress distribution in pelvis after ball head placement of prosthesis with different diameters. M0:the peak stress was 39.5 MPa after replacement of the original femoral head;M1:the peak stress was 47.3 MPa after replacement of the ball head with 48 mm diameter;M2:the peak stress was 54.2 MPa after replacement of the ball head with 49 mm diameter;M3:the peak stress was 44.8 MPa after replacement of the ball head with 47 mm diameter;M4:the peak stress was 50.2 MPa after replacement of the ball head with 46 mm diameter

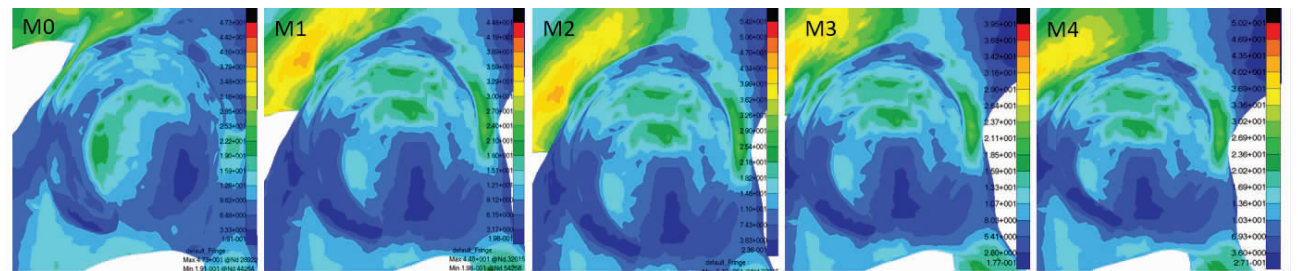


图 4 不同直径假体球头置入后髋臼 Von Mises 应力分布云图。M0:原股骨头置入时应力峰值为 22.2 MPa;M1:48 mm 球头置入时应力峰值为 24.0 MPa;M2:49 mm 球头置入时应力峰值为 20.1 MPa;M3:47 mm 球头置入时应力峰值为 23.3 MPa;M4:46 mm 球头置入时应力峰值为 25.1 MPa

Fig.4 Cloud chart of Von Mises stress distribution in acetabulum after ball head placement of prosthesis with different diameters. M0:the peak stress was 22.2 MPa after replacement of the original femoral head;M1:the peak stress was 24.0 MPa after replacement of the ball head with 48 mm diameter;M2:the peak stress was 20.1 MPa after replacement of the ball head with 49 mm diameter;M3:the peak stress was 23.3 MPa after replacement of the ball head with 47 mm diameter;M4:the peak stress was 25.1 MPa after replacement of the ball head with 46 mm diameter

而 M3(球头直径=47 mm)的应力峰值为 23.3 MPa,与术前最为接近,增量约 6.3%;其次是 M1(球头直径=48 mm),应力峰值为 24.0 MPa,增量约 8.1%。

同时由于人工股骨头置换术中并不处理髋臼软骨,本试验亦将髋臼软骨独立进行了 Von Mises 应力分析。根据图 5 可见,随假体球头直径增大或减小,髋臼软骨上出现弧形应力集中区,并对应着向外围或内圈移动,M2(球头直径=49 mm)由于球头直径的增大,其月牙形软骨内圈应力分散,高应力区点状分布,欠均匀;M4(球头直径=46 mm)由于球头直径的减小,软骨内圈呈现应力集中且面积显著增加。其中 M3(球头直径=47 mm)与 M1(球头直径=48 mm)应力分布同术前较相似,M3 的应力峰值为 18.5 MPa,最接近术前。

2.3 各模型股骨头的 Von Mises 应力分布

由图 6 可见,钴铬钼合金材料的人工股骨头弹

性模量远大于原股骨头的皮质骨,置换后的假体球头应力显著增加,应力集中区主要位于股骨头外上象限即与髋臼顶部相接触处,而在其下方则出现的不同程度的应力遮挡。四组模型中,M3(球头直径=47 mm)的应力遮挡区域面积及应力峰值最小,为 70.8 MPa。

3 讨论

髋臼磨损是人工股骨头置换术后常见的并发症,直接的临床表现为疼痛症状,可为钝痛、锐痛或剧烈刺痛不等,活动时加重,休息时缓解。疼痛部位多位于腹股沟或臀部,少数也会出现大腿痛,后者常在体位变化时,如坐位突然站起时发生。人工股骨头造成的髋臼磨损不同于全髋置换松动造成的骨缺损^[7-8],即较单纯的软骨、骨与金属的磨损,一般为空洞状缺损或者穿透内壁的复合缺损。造成髋臼磨损主要由患者自身及假体本身这两方面引起,前者包

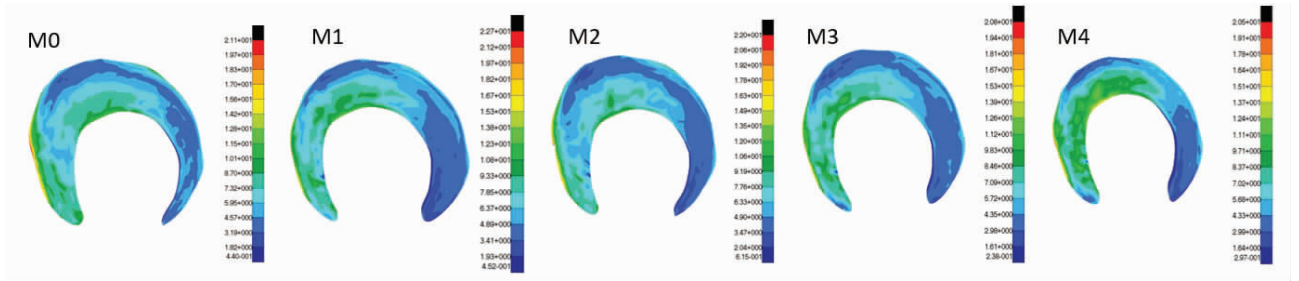


图 5 不同直径假体球头置入后髋臼软骨 Von Mises 应力分布云图 M0:原股骨头置入时应力峰值为 18.2 MPa;M1:48 mm 球头置入时应力峰值为 22.5 MPa;M2:49 mm 球头置入时应力峰值为 25.4 MPa;M3:47 mm 球头置入时应力峰值为 18.5 MPa;M4:46 mm 球头置入时应力峰值为 22.9 MPa

Fig.5 Cloud chart of Von Mises stress distribution in acetabular cartilage after ball head placement of prosthesis with different diameters. M0:the peak stress was 18.2 MPa after replacement of the original femoral head;M1:the peak stress was 22.5 MPa after replacement of the ball head with 48 mm diameter;M2:the peak stress was 25.4 MPa after replacement of the ball head with 49 mm diameter;M3:the peak stress was 18.5 MPa after replacement of the ball head with 47 mm diameter;M4:the peak stress was 22.9 MPa after replacement of the ball head with 46 mm diameter

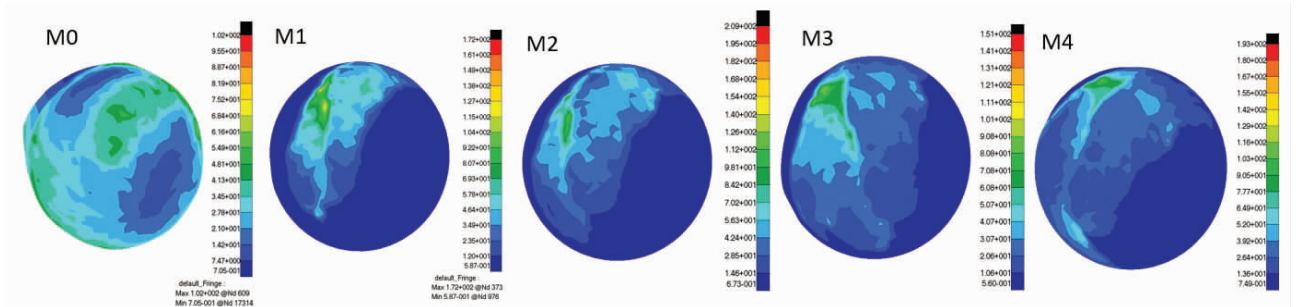


图 6 不同直径假体球头置入后假体球头 Von Mises 应力分布云图 M0: 原股骨头置入时应力峰值为 54.9 MPa;M1:48 mm 球头置入时应力峰值为 80.7 MPa;M2:49 mm 球头置入时应力峰值为 98.1 MPa;M3:47 mm 球头置入时应力峰值为 70.8 MPa;M4:46 mm 球头置入时应力峰值为 90.5 MPa

Fig.6 Cloud chart of Von Mises stress distribution in prosthetic head after ball head placement of prosthesis with different diameters. M0:the peak stress was 54.9 MPa after replacement of the original femoral head;M1:the peak stress was 80.7 MPa after replacement of the ball head with 48 mm diameter; M2:the peak stress was 98.1 MPa after replacement of the ball head with 49 mm diameter;M3:the peak stress was 70.8 MPa after replacement of the ball head with 47 mm diameter;M4:the peak stress was 90.5 MPa after replacement of the ball head with 46 mm diameter

括患者年龄、体重、活动量等；而后者包括髋臼-球头的摩擦以及人工股骨头直径等。

既往对假体球头直径的研究大部分是在全髋关节置换术中，人工股骨头置换术中假体球头直径的选择以往关注较少，随着人工股骨头置换术基数及术后髋臼磨损等并发症的病例数不断增加，学者们回过头来探讨其原因，发现假体球头直径在半髋置换术中也是一项重要的因素，而且会对患者的术后功能产生一定影响，因此在临床上也被重视起来。但由于这一问题提出较晚，术中假体球头的直径也多是笼统地选择与原股骨头直径相似进行安装，缺乏精确的指导。

目前对于假体球头过大或过小到底何者更易导致髋臼磨损并未达成一致。Wu 等^[9]通过计算机模拟研究了人工髋关节的磨损行为，验证了较大的股骨头可能导致较大的磨损量，但磨损深度较小，且磨损深度和体积损失与股骨头直径呈明显的非线性关

系。Schiavina 等^[10]对 209 例术后 10 年的随访病例根据球头直径大于或小于 48 mm 分为两组，进行多变量分析得出股骨头直径是髋臼磨损的唯一相关因素，且较小的头部尺寸更导致磨损加剧。

髋臼与股骨头之间的摩擦不可避免的，要减少这种摩擦，选择大小合适的股骨头假体非常重要。Squires 等^[11]研究者发现 2 mm 的头-臼误差会产生 66% 的髋臼磨损并导致 36% 的后期翻修率。李强等^[12]对 56 例因股骨颈骨折行人工股骨头置换的病例长达 9 年的临床随访发现，若患者股骨头直径在假体头直径 2 个型号（相差 2 mm）之内，可明显减少髋臼磨损的发生。Cabanela 等^[13]研究显示试模时假体头直径若以 1 mm 递增，可以改善匹配程度并减低髋臼的磨损程度。

目前多数学者及研究所秉持的原则是：手术所取下的股骨头与人工假体头两者所测量的直径不应该超过 2 mm，宁小勿大^[14]。但是现并无严格的生物

力学试验来验证不同直径假体球头对髋关节生物力学特别是髋臼磨损的影响。

试验中,正常生理情况下骨盆没有明显的应力集中情况。当对髋关节配以不同直径假体球头后,各模型中髌骨翼下方坐骨大切迹处均出现了不同程度的应力集中, M2 及 M4 的增幅位列前 2 位。由此可见,选择过大或过小的假体球头安装于髋臼中,其通过骨盆力学传导途径^[15],均会产生较大的应力集中,导致该区域骨吸收快于骨形成,造成骨质减少,如果超过骨的屈服极限,则最终引发局部骨质的机械性结构破坏。

另外,由于手术对髋关节囊、孟唇的影响,或是假体置换后股骨偏心矩的改变以及术后外展肌力的减弱,可使 M1-M4 髋臼区域应力峰值的位置由臼顶部后上方转为臼顶部上方。且推测由于原股骨头存在股骨头凹,而人工股骨头为光滑半球体,所以在髋臼中心区亦出现不同程度的应力集中。如结果显示,过大的假体球头与髋臼窝匹配度并不佳,出现的应力遮可致骨形成大于骨吸收^[16-17],造成臼缘骨质增生,关节间隙减小,摩擦面积增加,从而加速磨损的发生,并诱发早期的髋关节疼痛或活动受限,最后导致髋关节骨性关节炎的发生。而过小的假体球头缺乏臼窝对其的包容度,在中心区出现的应力集中可导致该区域骨吸收加快,磨损受力不均的软骨内侧缘,增加了假体不稳甚至中心性脱位的风险。

由此总结,不同直径的假体球头对人工股骨头置换术后的髋关节可产生不同的应力变化。在行人工股骨头置换术时,建议优先使用比原股骨头直径小 1 mm 的假体球头,其次是与原股骨头直径相等的假体球头,来获得与置换术前的髋关节最接近的自然力学特性,降低因尺寸差异导致的并发症风险。

参考文献

- [1] Zhao YQ, Fu D, Chen K, et al. Outcome of hemiarthroplasty and total hip replacement for active elderly patients with displaced femoral neck fractures: a meta-analysis of 8 randomized clinical trials[J]. PLoS One, 2014, 9(5): e98071.
- [2] Jmsen E, Eskelinen A, Peltola M, et al. High early failure rate after cementless hip replacement in the octogenarian[J]. Clin Orthop Relat Res, 2014, 472(9): 2779-2789.
- [3] Sheth NP, Dattilo JR, Schwarzkopf R. Evaluation and management of failed hemiarthroplasty[J]. J Am Acad Orthop Surg, 2018, 26(20): 717-726.
- [4] 张绍伟, 彭李华, 赵光荣, 等. 人工股骨头置换治疗骨质疏松股骨转子间不稳定骨折的有限元应力分析[J]. 中国组织工程研究与临床康复, 2011, 15(35): 6496-6499.
- [5] Polikeit A, Nolte LP, Ferguson SJ. The effect of cement augmentation on the load transfer in an osteoporotic functional spinal unit: finite-element analysis[J]. Spine (Phila Pa 1976), 2003, 28(10): 991-996.
- [6] Wei HW, Sun SS, Eric Jao SH, et al. The influence of mechanical properties of subchondral plate, femoral head and neck on dynamic stress distribution of the articular cartilage[J]. Med Eng Phys, 2005, 27(4): 295-304.
- [7] 蒋营军, 吴连国. 人工关节置换术后磨损颗粒与假体周围骨溶解的研究进展[J]. 中国骨伤, 2016, 30(10): 968-972.
- [8] Teeter MG, Lanting BA, Naudie DD, et al. Highly crosslinked polyethylene wear rates and acetabular component orientation: A minimum ten-year follow-up[J]. Bone Joint J, 2018, 100B(7): 891-897.
- [9] Wu JSS, Hung JP, Shu CS, et al. The computer simulation of wear behavior appearing in total hip prosthesis[J]. Comput Methods Programs Biomed, 2003, 70(1): 81-91.
- [10] Schiavina P, Pogliacomi F, Colombo M, et al. Acetabular erosion following bipolar hemiarthroplasty: A role for the size of femoral head[J]. Injury, 2019, 50(Suppl 4): 21-25.
- [11] Squires B, Bannister G. Displaced intracapsular neck of femur fractures in mobile independent patients: total hip replacement or hemiarthroplasty[J]. Injury, 1999, 30(5): 345-348.
- [12] 李强, 王志义, 朱光宇. 单极人工股骨头置换的中远期疗效分析[J]. 中华骨科杂志, 2005, 25(7): 395-399.
- [13] Cabanela ME. Bipolar versus total hip arthroplasty for avascular necrosis of the femoral head[J]. Clin Orthop Relat Res, 1990, (261): 59-62.
- [14] Vafaiean B, Zonoobi D, Mabee M, et al. Finite element analysis of mechanical behavior of human dysplastic hip joints: a systematic review[J]. Osteoarthritis Cartilage, 2017, 25(4): 438-447.
- [15] 张海峰, 尹爱华, 董毅. 有限元法分析不同负荷下髋臼区的应力分布[J]. 中国组织工程研究, 2016, 20(39): 5867-5872.
- [16] ZHANG HF, YIN AH, DONG Y. Finite element analysis of stress distribution in acetabulum under different loads[J]. Zhongguo Zu Zhi Gong Cheng Yan Jiu, 2016, 20(39): 5867-5872. Chinese.
- [17] Lavigne M, Laffosse JM, Ganapathi M, et al. Residual groin pain at a minimum of two years after metal-on-metal THA with a twenty-eight-millimeter femoral head, THA with a large-diameter femoral head, and hip resurfacing[J]. J Bone Joint Surg Am, 2011, 93(Suppl 2): 93-98.
- [18] Butterwick D, Papp S, Gofton W, et al. Acetabular fractures in the elderly: evaluation and management[J]. J Bone Joint Surg Am, 2015, 97(9): 758-768.